Binding Affinities of Synthetic Peptides, Pyridine-2-carboxamidonetropsin and 1-Methylimidazole-2-carboxamidonetropsin, That Form 2:1 Complexes in the Minor Groove of Double-Helical DNA†

Warren S. Wade, Milan Mrksich, and Peter B. Dervan*

Arnold and Mabel Beckman Laboratories of Chemical Synthesis, California Institute of Technology, Pasadena, California 91125

Received May 26, 1993; Revised Manuscript Received August 9, 1993®

ABSTRACT: The designed peptides pyridine-2-carboxamidonetropsin (2-PyN) and 1-methylimidazole-2-carboxamidonetropsin (2-ImN) are crescent-shaped analogs of the natural products netropsin and distamycin A. 2-PyN and 2-ImN bind the 5′-TGTCA-3′ sequence as antiparallel side-by-side dimers in the minor groove of DNA. The binding affinities of 2-PyN and 2-ImN to four different 5-bp sites on DNA were determined by quantitative MPE·Fe(II) footprint titration and compared with the tripeptide D from distamycin. The binding affinities of D to the sites 5′-TTTTT-3′ and 5′-TGTCA-3′ are 2.6×10^7 and $<1 \times 10^5$ M^{-1}, respectively (pH 7.0, 100 mM NaCl). 2-PyN binds these sites with similar affinities, 2.3×10^5 and 2.7×10^5 M^{-1}, respectively. The affinities of 2-ImN to the same two sites are $<5 \times 10^4$ and 1.4×10^5 M^{-1}, respectively. Substitution of an *N*-methylpyrrole-2-carboxamide of the distamycin tripeptide by 1-methylimidazole-2-carboxamide has changed the specificities for the two binding sites by a factor of 10^3. The data for 2-PyN and 2-ImN binding the 5′-TGTCA-3′ site are best fit by a cooperative binding curve consistent with 2:1 peptide–DNA complexes.

Netropsin and distamycin A are natural products that bind in the minor groove of double-helical DNA at sites of four or five successive A·T base pairs [for reviews, see Zimmer and Wähnert (1986) and Dervan (1986)]. X-ray (Kopka et al., 1985a,b; Coll et al., 1987) and NMR (Patel & Shapiro, 1986; Klevitt et al., 1986; Pelton & Wemmer, 1988) studies of netropsin– and distamycin–DNA complexes reveal how sequence specificity is accomplished. The crescent-shaped di- and tripeptides are bound in the center of the minor groove, allowing the amide hydrogens of the *N*-methylpyrrolecarboxamides to form bifurcated hydrogen bonds with the adenine N3 and thymine O2 atoms on the floor of the minor groove. The pyrrole rings fill the groove completely and form extensive van der Waals contacts with the walls and floor of the minor groove. The aromatic hydrogens of the *N*-methylpyrrole rings are set too deeply in the minor groove to allow room for the guanine amino group of a G·C base pair, affording binding specificity for A·T sequences.

Binding isotherms reveal that for both netropsin and distamycin binding A·T-rich DNA, the binding affinities are high and qualitatively similar ($\Delta G°$ = –12 kcal/mol) for complexation to poly[d(A-T)]·poly[d(A-T)] and poly(dA)·poly(dT) (Breslauer et al., 1987). The origins for these stabilities are, however, quite different. Binding to the alternating copolymer duplex by the peptides is enthalpy driven, whereas binding to the homopolymer duplex is entropy driven. Moreover, not all 5-bp[1] A·T-rich sites are bound with equal affinity. From footprinting experiments, a distamycin analog (D) containing the tripeptide unit tris(*N*-methylpyrrolecarboxamide) binds to 5-bp A·T-rich sites in the order of decreasing affinity 5′-TTTTT-3′ > 5′-AATAA-3′ > 5′-TTAAT-3′ (Wade et al., 1992).

In an effort to alter the sequence specificity of the natural product distamycin, pyridine-2-carboxamidonetropsin (2-PyN) and 1-methylimidazole-2-carboxamidonetropsin (2-ImN) were synthesized wherein the terminal *N*-methylpyrrolecarboxamide was replaced by a pyridine-2-carboxamide or 1-methylimidazole-2-carboxamide (Wade & Dervan, 1987; Wade et al., 1992) (Figure 1). Footprinting experiments indicate that 2-PyN binds the 5-bp sequences with altered specificity in the order of decreasing affinity 5′-TTTTT-3′ ~ 5′-TGTCA-3′ > 5′-TTAAT-3′ ~ 5′-AATAA-3′ (Wade & Dervan, 1987; Wade et al., 1992). Remarkably, 2-ImN preferentially binds to the 5′-TGTCA-3′ site (Wade et al., 1992). Direct structural characterization of the $(2\text{-PyN})_2$·5′-TGACT-3′ and $(2\text{-ImN})_2$·5′-TGACT-3′ complexes by two-dimensional NMR spectroscopy shows that both 2-PyN and 2-ImN bind as antiparallel side-by-side dimers in the minor groove (Figures 2C and 2D) (Mrksich et al., 1992; Dwyer et al., 1993).

Measurement of the energetics of a series of 1:1 and 2:1 peptide–DNA complexes is an important component for elucidating general design principles for the sequence-specific recognition of DNA in the minor groove. We describe here quantitative footprint titrations to measure equilibrium association constants for three peptides at four different 5-bp sites (Figure 3). Because the 5-bp binding sites are closely spaced, we utilize the high-resolution footprinting reagent methidiumpropyl-EDTA·Fe(II) (MPE·Fe(II)) (Hertzberg & Dervan, 1982, 1984; Van Dyke et al., 1982; Van Dyke & Dervan, 1983).

† We are grateful to the National Institutes of Health (GM-27681) and Burroughs Wellcome for research support, a National Science Foundation predoctoral fellowship to W.S.W., and a National Institutes of Health Research Service Award to M.M.

* To whom correspondence should be addressed.

® Abstract published in *Advance ACS Abstracts,* October 1, 1993.

[1] Abbreviations: bp, base pairs; D, tris(*N*-methylpyrrole-2-carboxamide); 2-PyN, pyridine-2-carboxamidonetropsin; 2-ImN, 1-methylimidazole-2-carboxamidonetropsin; MPE·Fe(II), methidiumpropyl-EDTA·Fe(II).

0006-2960/93/0432-11385$04.00/0

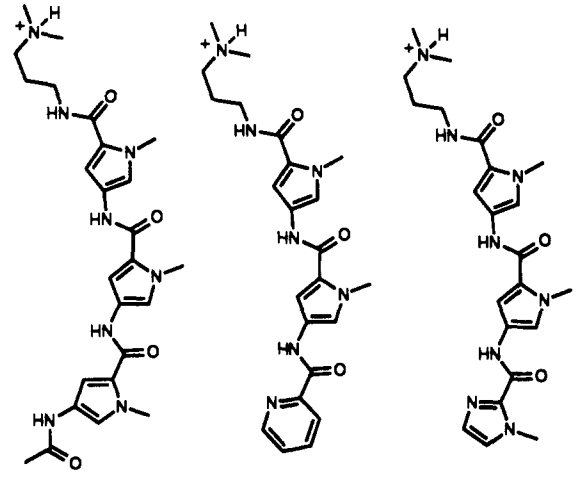

FIGURE 1: Synthetic peptides D, 2-PyN, and 2-ImN.

MATERIALS AND METHODS

Materials and DNA Preparation. The distamycin analog D and the designed peptides 2-PyN and 2-ImN were synthesized as previously reported (Taylor et al., 1984; Wade et al., 1992). The labeled 517-bp *Eco*RI/*Rsa*I restriction fragment of pBR322 was prepared by using standard methods with two modifications (Sambrook et al., 1989). The linearized plasmid was labeled at the 3′ end using both [α-^{32}P]dATP and [α-^{32}P]TTP. After ethanol precipitation, the labeled fragment was resuspended in 100 μL of 20 mM Tris·HCl, pH 7, and diluted to 2 mL with water. The solution was concentrated using an Amicon Centricon 30 000 MW cutoff membrane, diluted to 4000 cpm/μL, and stored at −20 °C. Typically, each labeled fragment contained 3–4 radioactive nucleotides. Adenine-specific chemical sequencing reactions were performed as described by Iverson and Dervan (1987).

Quantitative MPE·Fe(II) Footprint Titrations. Into 1.5-mL Eppendorf tubes were placed 160 μL of 1.25× buffer (25 mM Tris·HCl, 125 mM NaCl, pH 7.0) and 10 μL of a 50-bp μM poly(dG)·poly(dC) solution containing 30 000 cpm 3′-labeled 517-bp restriction fragment. The peptide to be footprinted was serially diluted, and 20 μL of the appropriate concentration solution was added to each tube. The tubes were mixed and incubated at 37 °C for 30 min. Five microliters of a freshly prepared 80 mM dithiothreitol (DTT) solution and 5 μL of a 40 μM MPE·Fe(II) solution in separate drops were added, and the reactions were mixed and incubated at 37 °C for 10 min. Twenty-five microliters of a 40 μg/mL tRNA solution and 700 μL of ethanol were added, and the reactions were precipitated without added salt, counted, and diluted to 3000 cpm/μL with formamide buffer. All samples were loaded in wells separated by 6 mm and electrophoresed on 8% polyacrylamide denaturing gels (5% cross-link, 7 M urea). The gels were dried and exposed to preflashed X-ray film at −78 °C with one intensifying screen.

Modifications for Small Molecule Footprint Titrations. In order to use the procedure described by Ackers and coworkers (Brenowitz et al., 1986; Senear et al., 1986) to determine small molecule–DNA binding constants at closely-spaced distinct sites on DNA restriction fragments, the intercalator methidiumpropyl-EDTA·Fe(II) (MPE·Fe(II)) is used as the footprinting agent (Ward et al., 1988; Dabrowiak & Goodisman, 1989; Dabrowiak et al., 1990; Hertzberg & Dervan, 1982, 1984; Van Dyke et al., 1982; Van Dyke & Dervan, 1983). It is important that determinations of peptide binding constants are not affected by peptide binding to nearby

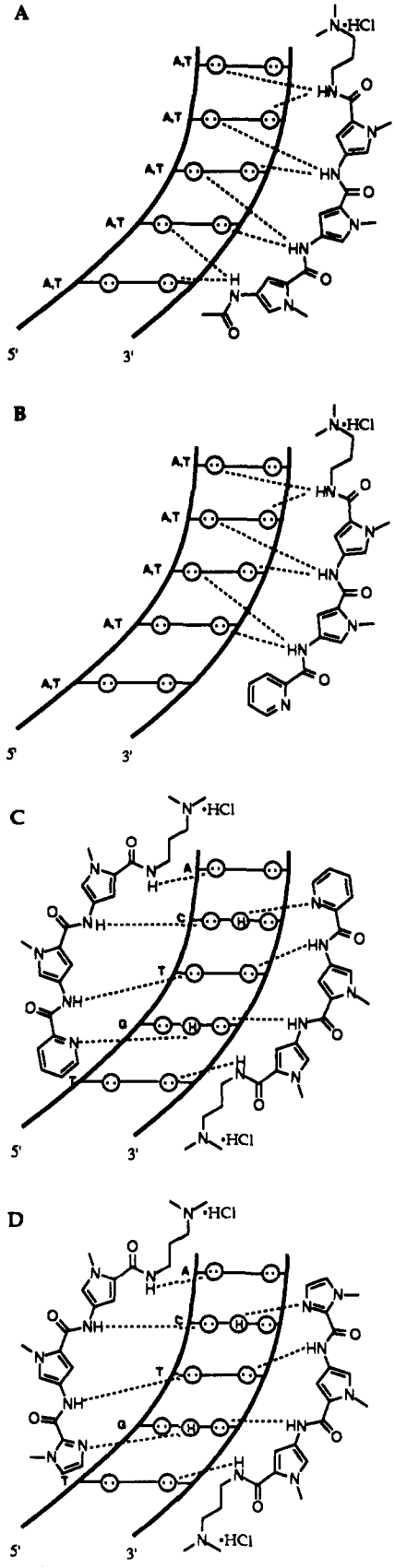

FIGURE 2: 1:1 Binding models for the complexes formed between (A) D with a 5′-(A·T)$_5$-3′ sequence and (B) 2-PyN with a 5′-(A·T)$_5$-3′ sequence, with the nitrogen of the pyridine facing away from the minor groove. 2:1 Binding models for the dimeric complexes formed between (C) 2-PyN with a 5′-TGTCA-3′ sequence, with the nitrogens of the pyridines facing toward the floor of the minor groove, and (D) 2-ImN with a 5′-TGTCA-3′ sequence. Circles with dots represent lone pairs of N3 of purines and O2 of pyrimidines and circles with an H represent the 2-amino group of guanine. Putative hydrogen bonds are illustrated by dashed lines.

(A) D

5'-GCCTATTTTTATAGCTTAATGTCATGATAATAATGG-3'
3'-CGGATAAAAATATCCAATTACAGTACTATTATTACC-5'

(B) 2-PyN

5'-GCCTATTTTTATAGCTTAATGTCATGATAATAATGG-3'
3'-CGGATAAAAATATCCAATTACAGTACTATTATTACC-5'

(C) 2-ImN

5'-GCCTATTTTTATAGCTTAATGTCATGATAATAATGG-3'
3'-CGGATAAAAATATCCAATTACAGTACTATTATTACC-5'

FIGURE 3: Binding sites for which apparent first-order binding affinities were determined. (A) D in complex with A·T-rich sites; (B) 2-PyN in complex with A·T-rich sites and the 5'-TGTCA-3' site; and (C) 2-ImN in complex with the 5'-TGTCA-3' site.

sites. The MPE·Fe(II) cleavage patterns 3 bases away from occupied binding sites are essentially normal, suggesting that independent binding affinities can be determined. The use of this relatively non-sequence-specific DNA cleavage reagent gives a Poisson distribution of DNA fragments and results in no significant degradation of the DNA-binding ligand (Van Dyke et al., 1982; Van Dyke & Dervan, 1983). Because 90% of the added MPE·Fe(II) is free in solution under normal footprinting conditions, cleavage enhancement at sites not bound by the ligand is usually not observed (Hertzberg & Dervan, 1984). In a footprinting experiment, >99% of the DNA is nonradioactive carrier. Poly(dG)·poly(dC) was used as the carrier DNA since D, 2-PyN, and 2-ImN do not bind G·C-rich sequences at 50 μM concentrations (Wade et al., 1992).

Calculation of Fraction Bound. A suitable autoradiogram was scanned over the width of each lane using an LKB Ultrascan XL laser densitometer. Data analysis was performed using GSXL software (LKB) running on an IBM AT computer. The peaks for each lane were integrated after the data were corrected for background variability by subtracting an average of the two 1-mm base-line scans from either side of the lane in question. The apparent fractions bound (θ_{app}) were calculated as described by Brenowitz et al. (1986). In

$$\theta_{app} = 1 - \frac{OD_{site}/OD_{ref}}{OD_{site,std}/OD_{ref,std}} \quad (1)$$

eq 1, OD_{site} and OD_{ref} refer to the amounts of digestion at the target site and at the reference site, respectively. $OD_{ref,std}$ and $OD_{site,std}$ refer to the amounts of digestion at these same sites in a MPE·Fe(II) control to which no peptide was added. For 2-PyN and 2-ImN, a 5'-CCG-3' sequence was chosen as the reference, and for D, the 5'-TCA-3' sequence that shows the minimum protection was chosen as the reference. Average θ_{app} values were determined from at least three independent gels. Different samples of the small molecule were used on each gel, with at least two different labelings in each set of three or four experiments, and at least two different MPE·Fe(II) samples in each set. Binding affinities were determined for each set of experiments after the θ_{app} values were averaged.

Fitting Procedure. A Langmuir binding titration isotherm (eq 2) was fit to the ([L], θ_{app}) data points using the θ-value at saturation binding (θ_{max}), the θ-value at no binding (θ_{min}), and the K_a as adjustable parameters. The difference between θ_{fit} and θ_{app} for all ([L], θ_{app}) data points is minimized using a gradient procedure combined with a linear expansion of the

$$\theta_{fit} = (\theta_{max} - \theta_{min})\frac{K_a[L]}{1 + K_a[L]} + \theta_{min} \quad (2)$$

function θ_{fit} as described by Marquardt (1963) and implemented by Bevington (1969). The goodness of fit of the binding curve to the data points is evaluated by the reduced χ^2 criterion (Bevington, 1969). Fits are judged acceptable if the χ_ν^2 at a site other than the 5'-TTTTT-3' site is 1.5 or less.

Binding to the 5'-TGTCA-3' Site. The best-fit binding isotherms for 2-ImN and 2-PyN binding to the 5'-TGTCA-3' site consistently give much worse fits than the other complexes. Visual inspection of the binding curves reveals that, in both cases, the increase in θ_{app} near half-saturation of the site is steeper than expected from the fitted curve, consistent with cooperative dimeric binding to this sequence by the peptides. While NMR and affinity cleaving experiments reveal that the peptides bind with positive cooperativity, the degree of cooperativity cannot be inferred from these experiments (Mrksich et al., 1992; Wade et al., 1992). Moreover, these experiments cannot distinguish between binding by preassociated dimers and stepwise binding by two free peptides. It is likely that the footprinting data presented here also cannot distinguish between these possible mechanisms. In considerations of a preassociation binding mechanism, the ([L], θ_{app}) data points were fit to eq 3:

$$\theta_{fit} = (\theta_{max} - \theta_{min}) \times \frac{K_B(1 + 4K_D[L] - \sqrt{1 + 8K_D[L]})}{8K_D + K_B(1 + 4K_D[L] - \sqrt{1 + 8K_D[L]})} + \theta_{min} \quad (3)$$

where K_D corresponds to the dimerization constant for the peptides and K_B corresponds to the association constant of the peptide dimer with the DNA site. Nonlinear least-squares analysis with K_D, K_B, θ_{min}, and θ_{max} as adjustable parameters resulted in good fits but with large variability in the K_D and K_B parameters. Fitted values for K_D ranged from 10 to 1000 M^{-1}, and those for K_B ranged from 10^7 to 10^9 M^{-1}. In consideration of a stepwise binding mechanism, the same data were fit to eq 4:

$$\theta_{fit} = (\theta_{max} - \theta_{min})\frac{K_1[L] + K_1K_2[L]^2}{1 + K_1[L] + K_1K_2[L]^2} + \theta_{min} \quad (4)$$

where K_1 corresponds to the association constant for binding of the first peptide and K_2 to the association constant for binding of the second peptide to a singly occupied site. Nonlinear least-squares analysis using eq 4 with K_1, K_2, θ_{min}, and θ_{max} as adjustable parameters also produced fits of good quality. In the cases of both 2-PyN and 2-ImN binding to this sequence, we find $K_2 > K_1$, with the K_2/K_1 ratios ranging from 10 to 300. Clearly, the data are not of sufficient precision to allow for accurate independent determination of the two stepwise binding constants. Therefore, we chose to fit the data to a cooperative binding curve (eq 5) with K_a, θ_{min}, θ_{max}, and n as adjustable parameters. In fact, in the case of $K_2 \gg$

$$\theta_{fit} = (\theta_{max} - \theta_{min})\frac{K_a^n[L]^n}{1 + K_a^n[L]^n} + \theta_{min} \quad (5)$$

K_1, eq 4 is approximately equivalent to eq 5, with $K_1K_2 \approx K_a^2$. We note explicitly that treatment of the data in this manner does not represent an attempt to model a binding mechanism. Rather, we have chosen to compare values of K_a, the apparent first-order binding affinity, because this parameter represents the concentration of peptide at which the binding site is half-saturated.

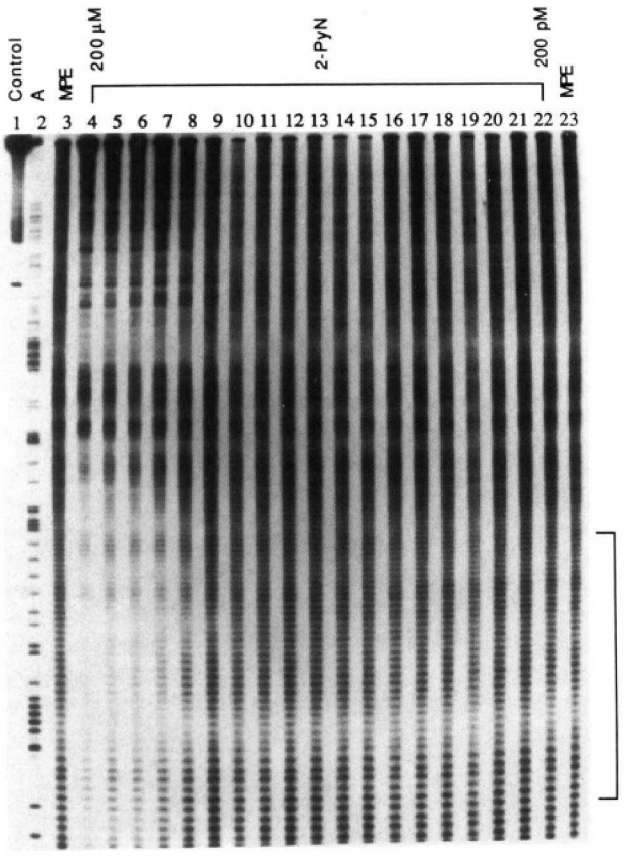

FIGURE 4: Autoradiogram of an 8% polyacrylamide gel used to separate the products generated by MPE·Fe(II) digestion during a quantitative footprint titration using 2-PyN. All reactions contain 2 mM DTT, 2.5 μM-bp poly(dG)·poly(dC), and 12 kcpm of 3′-labeled 517-bp restriction fragment in 40 mM Tris·HCl, 100 mM sodium chloride, pH 7.0 buffer. Lane 1, intact DNA; lane 2, A reaction. Lanes 3–23 contain 1 μM MPE·Fe(II): lanes 3 and 23 are MPE·Fe(II) standards; lanes 4–22 contain 200 μM, 100 μM, 50 μM, 20 μM, 10 μM, 5 μM, 2 μM, 1 μM, 500 nM, 200 nM, 100, nM, 50 nM, 20 nM, 10 nM, 5 nM, 2 nM, 1 nM, 500 pM, and 200 pM 2-PyN, respectively.

Table I: Apparent First-Order Affinity Constants (M^{-1})[a,b]

	binding site			
peptide	5′-TTTTT-3′	5′-TTAAT-3′	5′-TGTCA-3′	5′-AATAA-3′
D	2.6×10^7 (1.8)	1.9×10^6 (0.8)	$<1 \times 10^5$	1.4×10^7 (0.9)
2-PyN	2.3×10^5 (1.2)	6.9×10^4 (1.6)	2.7×10^5 (0.3)	5.4×10^4 (0.4)
2-ImN	$<5 \times 10^4$	$<1 \times 10^4$	1.4×10^5 (0.3)	$<2 \times 10^4$

[a] Determined from average θ_{app} values from three gels (standard deviation for three independent determinations from single gels). [b] 20 mM Tris·HCl, pH 7.0, 100 mM NaCl.

RESULTS

Binding Affinities. Quantitative MPE·Fe(II) footprint titration experiments with the three peptides D, 2-PyN, and 2-ImN binding to the four sites 5′-TTTTT-3′, 5′-TTAAT-3′, 5′-TGTCA-3′, and 5′-AATAA-3′ reveal that these peptides display very different sequence specificities (Figure 4). D binds to the three A·T-rich sites with apparent first-order binding affinities ranging from 1×10^6 to 3×10^7 M^{-1} (pH 7.0, 100 mM NaCl), with relative binding affinities in good agreement with previous qualitative studies (Table I). 2-PyN binds these A·T-rich sites with 100-fold lower affinities but with similar relative binding affinities. 2-PyN also binds the 5′-TGTCA-3′ site with comparable apparent affinity, affording little discrimination between the four sites. 2-ImN, however, preferentially binds the 5′-TGTCA-3′ site, with similar binding affinity as does 2-PyN (Table I).

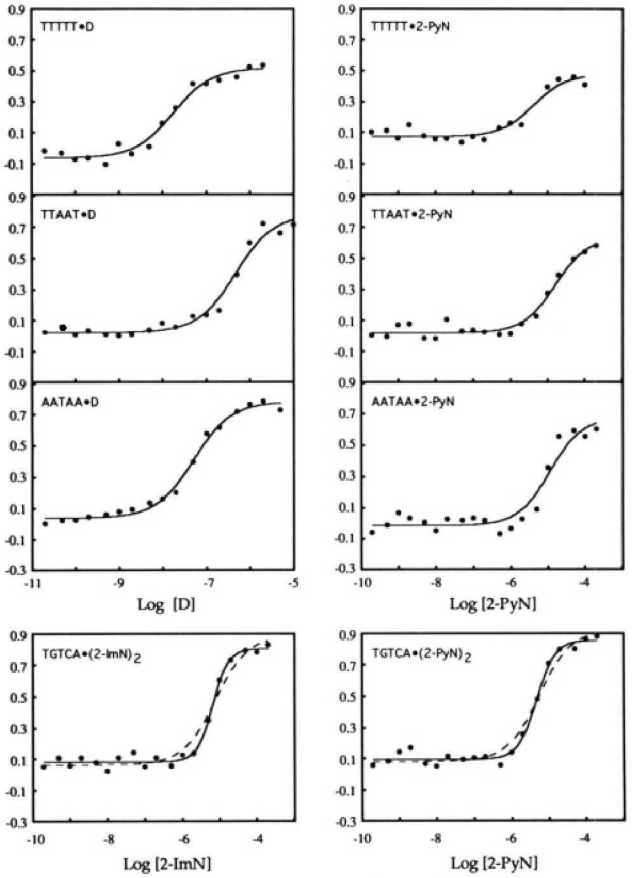

FIGURE 5: Data from quantitative MPE·Fe(II) footprint titration experiments for binding of D, 2-PyN, and 2-ImN to the sites 5′-TTTTT-3′, 5′-TTAAT-3′,5′-TGTCA-3′, and 5′-AATAA-3′. The DNA–peptide complex for each data set is noted at the upper left of each panel. The vertical axis represents the average θ_{app} value from three gels, with the θ_{app} data points represented as filled circles, and the solid curves are the best-fit Langmuir binding titration isotherms for each data set. Binding isotherms for 2-PyN and 2-ImN in complex with the 5′-TGTCA-3′ site were determined with a cooperative model and are represented as the solid curves. Also shown for these complexes are the best-fit Langmuir binding isotherms as dashed curves (from eq 2, see Materials and Methods for details).

1:1 and 2:1 Complexes. While the ($[L]$, θ_{app}) data points for D and 2-PyN in complex with the three A·T-rich sites can be adequately described with a simple 1:1 Langmuir binding isotherm (eq 2), the fits were significantly worse for 2-ImN and 2-PyN in complex with the 5′-TGTCA-3′ site. The steepness of the ($[L]$, θ_{app}) data points could be satisfactorily accounted for using a stepwise binding equation (eq 4). Although the results of curve-fitting using this equation were consistent with a high degree of cooperativity in the binding of the second ligand, the error in determining the individual binding constants was large. The data were therefore fit to a cooperative binding curve with K_a, the apparent first-order association constant, θ_{min}, θ_{max}, and n as adjustable parameters (eq 5). For 2-PyN and 2-ImN binding the 5′-TGTCA-3′ site, the best-fit values of n are 1.9 and 2.0, respectively. Langmuir binding isotherms are superimposed on these best-fit isotherms in Figure 5, clearly demonstrating the more acceptable fit of the latter.

DISCUSSION

Binding to A·T-Rich Sites. D binds the three A·T-rich sites with apparent first-order affinity constants ranging from 1×10^6 to 3×10^7 M^{-1}. 2-PyN binds these three sites with binding affinities nearly 2 orders of magnitude lower than does D (Table I). Strong binding of D to A·T-rich sites has

been explained by a tight fit of the peptide in the minor groove and a complementary set of hydrogen bonds between the ligand and the floor of the minor groove. The amide NHs of D and 2-PyN can form an extended array of hydrogen bonds to the adenine N3 and thymine O2 atoms on the floor of the minor groove (Figures 2A and 2B). While the lower binding affinities of 2-PyN for A·T-rich sites can in part be explained by one less carboxamide NH for hydrogen bonding, the different geometries of pyridine and pyrrole rings may also be a contributing factor. 2-ImN does not bind these A·T-rich sites ($K_a < 10^5\ M^{-1}$). Unlike 2-PyN, 2-ImN is constrained to have a hydrogen bond acceptor atom facing the floor of the minor groove. The lack of a hydrogen bond donor for the peptide imidazole N3 atom and lone pair–lone pair charge repulsions presumably disfavor binding to A·T sequences and impart a large specificity for the mixed sequences.

Binding to the 5′-TGTCA-3′ Site. 2-PyN and 2-ImN bind to the 5′-TGTCA-3′ site with comparable affinities that are nearly 100-fold lower than that of D binding to A·T-rich sites. Since 2-PyN and 2-ImN bind the mixed sequence as side-by-side dimers, the lower association constants may reflect an entropic penalty. Consistent with this explanation, we have recently shown that covalently linking two peptides with alkyl tethers affords covalent peptides which bind with 10-fold higher affinities than do the nonlinked peptides (Mrksich & Dervan, 1993). Lower binding constants for G·C-containing sequences may also be a general consequence of sequence-dependent minor groove characteristics. If the guanine amino groups protruding from the floor of the minor groove do not allow the peptides to sit deeply in the minor groove, the peptides may bind with less favorable enthalpies and lower binding constants (Marky & Breslauer, 1987). 2-PyN and 2-ImN can accommodate the amino groups of the 5′-TGTCA-3′ site by participation in favorable hydrogen bonds with the peptide pyridine N1 and imidazole N3 nitrogens. The shallow penetration of the peptides in the minor groove forfeits the full benefit of the tight fit between peptide and DNA, resulting in lower binding affinities as compared to D in complex with A·T-rich sites. D, however, can neither participate in hydrogen bonds with the guanine amino groups nor be deeply set in the minor groove, resulting in low affinity for the mixed sequence 5′-TGTCA-3′.

In summary, removal of the *N*-terminal amide of D and replacement of a single aromatic CH by a nitrogen atom results in a change in relative specificity of over 3 orders of magnitude. This change is due in large part to alteration of the relative energetics of the two very different peptide–DNA complexes (1:1 versus 2:1 motif). With regard to ligand design, a chief determinant of binding motif, and hence sequence specificity, may be the minor groove width.

REFERENCES

Bevington, P. R. (1969) in *Data Reduction and Error Analysis for the Physical Sciences*, pp 204–245, McGraw Hill, New York.

Brenowitz, M., Senear, D. F., Shea, M. A., & Ackers, G. K. (1986) *Methods Enzymol. 130*, 133–181.

Breslauer, K. J., Remeta, D. P., Chou, W.-Y., Ferrante, R., Curry, J., Zaunczkowski, D., Snyder, J. G., & Marky, L. A. (1987) *Proc. Natl. Acad. U.S.A. 84*, 8922–8926.

Coll, M., Frederick, C. A., Wang, A. H.-J., & Rich, A. (1987) *Proc. Natl. Acad. Sci. U.S.A. 84*, 8385–8389.

Dabrowiak, J. C., & Goodisman, J. (1989) in *Chemistry & Physics of DNA-Ligand Interactions*, pp 143–174, Adenine Press, Guilderland, NY.

Dabrowiak, J. C., Goodisman, J., & Kissinger, K. (1990) *Biochemistry 29*, 6139–6145.

Dervan, P. B. (1986) *Science 232*, 464–471.

Dwyer, T. J., Geierstanger, B. H., Mrksich, M., Dervan, P. B., & Wemmer, D. E. (1993) *J. Am. Chem. Soc.* (in press).

Hertzberg, R. P., & Dervan, P. B. (1982) *J. Am. Chem. Soc. 104*, 313–315.

Hertzberg, R. P., & Dervan, P. B. (1984) *Biochemistry 23*, 3934–3945.

Iverson, B. L., & Dervan, P. B. (1987) *Nucleic Acids Res. 15*, 7823–7830.

Klevitt, R. E., Wemmer, D. E., & Reid, B. R. (1986) *Biochemistry 25*, 3296–3303.

Kopka, M. L., Yoon, C., Goodsell, D., Pjura, P., & Dickerson, R. E. (1985a) *Proc. Natl. Acad. Sci. U.S.A. 82*, 1376–1380.

Kopka, M. L., Yoon, C., Goodsell, D., Pjura, P., & Dickerson, R. E. (1985b) *J. Mol. Biol. 183*, 554–563.

Marky, L. A., & Breslauer, K. J. (1987) *Proc. Natl. Acad. Sci. U.S.A. 84*, 4359–4363.

Marquardt, D. W. (1963) *J. Soc. Ind. Appl. Math. 11*, 431–441.

Mrksich, M., & Dervan, P. B. (1993) *J. Am. Chem. Soc.* (in press).

Mrksich, M., Wade, W. S., Dwyer, T. J., Geierstanger, B. H., Wemmer, D. E., & Dervan, P. B. (1992) *Proc. Natl. Acad. Sci. U.S.A. 89*, 9586–9590.

Patel, D. J., & Shapiro, L. (1986) *J. Biol. Chem. 261*, 1230–1240.

Pelton, J. G., & Wemmer, D. E. (1988) *Biochemistry 27*, 8088–8096.

Sambrook, J., Fritsch, E. F., & Maniatis, T. (1989) in *Molecular Cloning: A Laboratory Manual*, Cold Spring Harbor Laboratory Press, Cold Spring Harbor, NY.

Senear, D. F., Brenowitz, M., Shea, M. A., & Ackers, G. K. (1986) *Biochemistry 25*, 7344–7354.

Taylor, J. S., Schultz, P. G., & Dervan, P. B. (1984) *Tetrahedron 40*, 457–465.

Van Dyke, M. W., & Dervan, P. B. (1983) *Nucleic Acids Res. 11*, 5555–5567.

Van Dyke, M. W., Hertzberg, R. P., & Dervan, P. B. (1982) *Proc. Natl. Acad. Sci. U.S.A. 79*, 5470–5474.

Wade, W. S. (1989) Ph.D. Thesis, California Institute of Technology, Pasadena, CA.

Wade, W. S., & Dervan, P. B. (1987) *J. Am. Chem. Soc. 109*, 1574–1575.

Wade, W. S., Mrksich, M., & Dervan, P. B. (1992) *J. Am. Chem. Soc. 114*, 8783–8794.

Ward, B., Rehfuss, R., Goodisman, J., & Dabrowiak, J. C. (1988) *Biochemistry 27*, 1198–1205.

Zimmer, C., & Wähnert, U. (1986) *Prog. Biophys. Mol. Biol. 47*, 31–122.